Journal of Materials Chemistry A

Accepted Manuscript

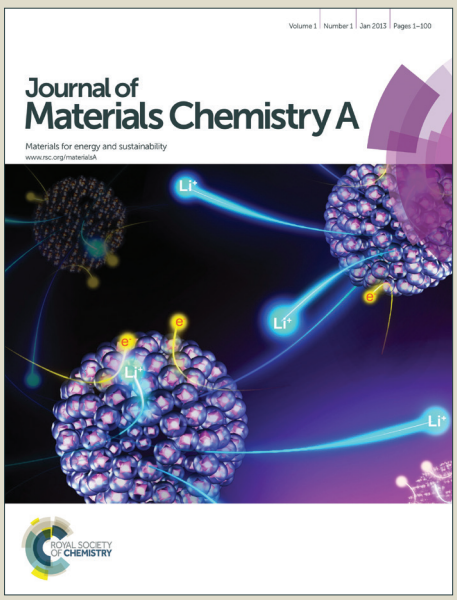

ROYAL SOCIETY OF CHEMISTRY

www.rsc.org/materialsA

Journal Name RSCPublishing

COMMUNICATION

Novel Visible-light Sensitive Vanadate Photocatalysts toward Water Oxidation: Implication from density functional theory calculations

Cite this: DOI: 10.1039/x0xx00000x

Received 00th January 2012,
Accepted 00th January 2012

DOI: 10.1039/x0xx00000x

www.rsc.org/

Peng Li[a] Naoto Umezawa[a,b,c]* Hideki Abe [a,b,c]* and Jinhua Ye [a,b,d]

Two vanadates, $Ag_2Sr(VO_3)_4$ and $Sr(VO_3)_2$, have been studied as visible-light-driven water oxidation photoctalysts with the help of density-functional theory calculations. Our computational results for density of states and partial charge densities implied that $Ag_2Sr(VO_3)_4$ and $Sr(VO_3)_2$ possess desirable electronic structures for water oxidation reaction, *i.e.*, the valence band (VB) maximum of $Ag_2Sr(VO_3)_4$ consists of multiple orbitals of Ag *d* and O *p*, while $Sr(VO_3)_2$ has a broad VB associated with oxygen non-bonding states. We have experimentally demonstrated that these vanadates efficiently oxidize water to O_2 under irradiation of visible light in the presence of the sacrificial agent.

For decades, photocatalysis has attracted more attention because of its great potential in converting solar energy into chemical fuels and/or in degradation of pollutants.[1-3] Among a series of applications, solar-light-driven water splitting has gained in importance as an ultimate solution to the current global energy crisis.[4-6] In order to realize direct water splitting by solar light using heterogeneous photocatalysts, suitable band gaps and band edge positions with respect to the water redox potentials are prerequisites. However, it is difficult to find a semiconductor with both of proper light absorption and high water splitting efficiency because narrow band-gap semiconductors can hardly provide sufficiently high redox energy to reduce and oxidize water simultaneously.[7, 8] As a result, separating the water splitting reaction in terms of two half-reactions, water reduction and water oxidation, is widely used to study the mechanism for the further development of overall water splitting photocatalyst.[9, 10]

A number of visible light responsive water oxidation photocatalysts have been previously reported, such as $BiVO_4$[11, 12] and Ag_3PO_4.[13-15] Detailed experimental- and theoretical studies were also carried out to understand the mechanism of their high water-oxidation activities.[14-16] The electronic structures in $BiVO_4$ and Ag_3PO_4 result in small effective masses of carriers which are advantageous for the carrier migration and photocatalytic reactions on the surface.[17, 18] In addition, the high performance of Ag_3PO_4 is partly attributed to the character of valence band maximum (VBM), with which hole carriers are mediated. In Ag_3PO_4, the VBM consists both of Ag *d*- and O *p* orbitals, and it is expected to provide a desirable platform for hole transportation through hopping process between Ag- and O atoms. In fact, mixing cation- and anion-originating states at VBM is a design principle for *p*-type semiconductors.[19] It was also found that oxygen vacancies (V_O), which are usually a source for *n*-type conductivity and eliminate hole carriers, if formed, are not a predominant defect in Ag_3PO_4[20] possibly because of the covalent nature in a PO_4 tetrahedra.[17] Hence we expect that an acid ligand such as VO_4^{3-} can also suppress the formation of V_O. For the above two reasons, we paid attention to $Ag_2Sr(VO_3)_4$ as a promising photocatalyst. Moreover, incorporation of Sr is expected to be beneficial for increasing in Madelung energy and stabilizing the silver-based oxides which are sensitive to photo-corrosion. We have also investigated the photocatalytic activity of $Sr(VO_3)_2$ for a comparison. Note that both $Ag_2Sr(VO_3)_4$ and $Sr(VO_3)_2$ are unexplored materials for photocatalytic water oxidation reaction.

According to a common observation of silver-based oxides, $Ag_2Sr(VO_3)_4$ is expected to possess a similar electronic structure with that of Ag_3PO_4, that is, its VBM consists both of Ag *d*- and O *p* states. The cation-anion hybrid nature of the VBM benefits the migration of photo-generated holes and may result in a possible activity of water oxidation. $Sr(VO_3)_2$ should have a totally different VBM because of the absence of silver atom. Interestingly, we have found that $Sr(VO_3)_2$ has a very high density of states at the VBM consisting of O non-bonding states forming a broad band, which can contribute to high performance in water oxidation reaction. To validate our theoretical implication, $Ag_2Sr(VO_3)_4$ and $Sr(VO_3)_2$ were synthesized by solid state reactions.[21] The photocatalytic O_2 evolution experiments showed that $Ag_2Sr(VO_3)_4$ and $Sr(VO_3)_2$ efficiently oxidize water into O_2 in the presence of sacrificial agent.

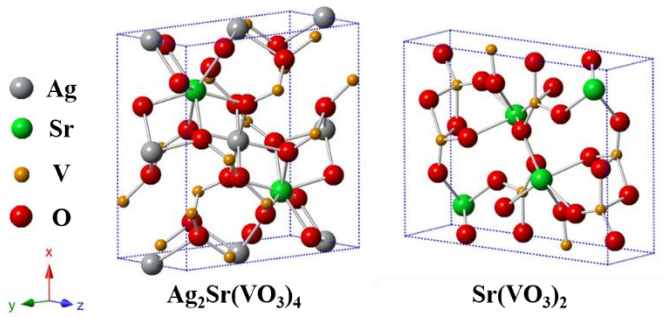

Figure 1. Schematic crystal structures of $Ag_2Sr(VO_3)_4$ and $Sr(VO_3)_2$.

Figure 1 presents schematic crystal structures of $Ag_2Sr(VO_3)_4$ and $Sr(VO_3)_2$. $Ag_2Sr(VO_3)_4$ has a tetragonal structure with the space group of *P4/nbm*, while $Sr(VO_3)_2$ crystallizes in an orthorhombic system with the space group of *Pnma*. Lattice parameters of these vanadates are listed in Table 1. Both of $Ag_2Sr(VO_3)_4$ and $Sr(VO_3)_2$ contain the same (VO_4) tetrahedron structures.

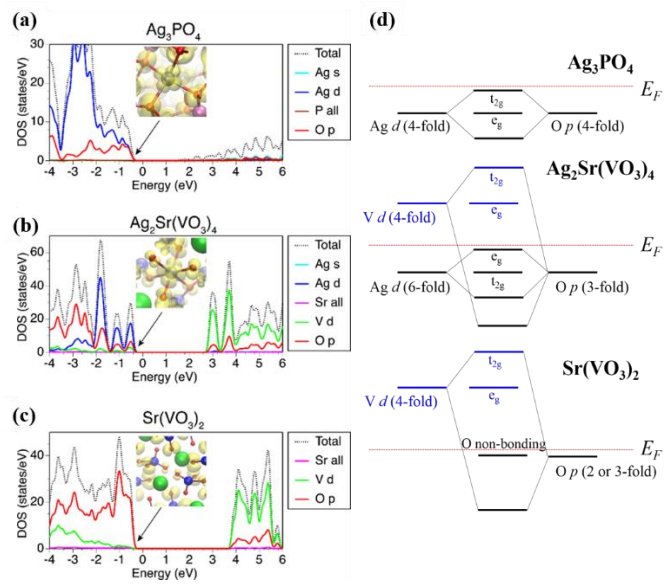

Figure 2. Total- and local density of states for (a) Ag_3PO_4, (b) $Ag_2Sr(VO_3)_4$ and (c) $Sr(VO_3)_2$. The insets in (a), (b), and (c) shows the corresponding VBM distributions. (d) Bond diagram of molecular orbitals for Ag_3PO_4, $Ag_2Sr(VO_3)_4$ and $Sr(VO_3)_2$.

Table 1. Lattice parameters for Ag_3PO_4, $Ag_2Sr(VO_3)_4$, and $Sr(VO_3)_2$ determined by our DFT calculations.

Materials		a (Å)	b (Å)	c (Å)
Ag_3PO_4	Theory	6.00	6.00	6.00
	Experiment[a]	6.00	6.00	6.00
$Ag_2Sr(VO_3)_4$	Theory	10.44	10.44	4.92
	Experiment[b]	10.6284(3)	10.6284(3)	4.9803(1)
$Sr(VO_3)_2$	Theory	9.60	3.62	12.47
	Experiment[c]	9.6740(1)	3.6847(1)	12.5614(2)

[a] Reference [22]
[b] This work, wRp = 0.0508, Rp = 0.0372
[c] This work, wRp = 0.0599, Rp = 0.0421

Figure 2b shows density of states for $Ag_2Sr(VO_3)_4$. As expected, the VBM is composed of multiple states of Ag *d*, O *p*, and V *d*. However, because of the strong *d*-character of Ag *d* state, the VBM in $Ag_2Sr(VO_3)_4$ consists of a narrow band, which is different from the broad band observed in the case of Ag_3PO_4 (Figure 2a). One structural difference between $Ag_2Sr(VO_3)_4$ and Ag_3PO_4 is in the coordination number of Ag atoms, *i.e.* Ag is 6-fold in $Ag_2Sr(VO_3)_4$, while it is 4-fold in Ag_3PO_4. This leads to the different *d*-character at the VBM as shown in the insets of Figure 2a and 2b, and schematically illustrated in Fig. 2d. The presence of Sr atoms, which have a large ionic radius, might also cause the isolation of Ag atoms inhibiting Ag *d* - O *p* hybridization. These are the major reasons for the formation of the undesirable narrow band at the VBM of $Ag_2Sr(VO_3)_4$. Hence, although one can expect that the oxidation reaction occurs on $Ag_2Sr(VO_3)_4$, its performance is not as high as that of Ag_3PO_4 as evidenced in our experiments discussed below. In $Sr(VO_3)_2$, some of O atoms are 2-fold, leading to the formation of abundant O non-bonding states near the VBM. The O non-bonding states are widely distributed as shown in the inset of Fig. 2c, contributing to the formation of a broad valence band (Fig. 2c). The difference in the bond formation among the three compounds is summarized in Figure 2d. It is likely that the formation of a broad abrupt band as well as the cation-anion mixed character at the VBM is an important materials-design principle for photocatalytic oxidation reactions.

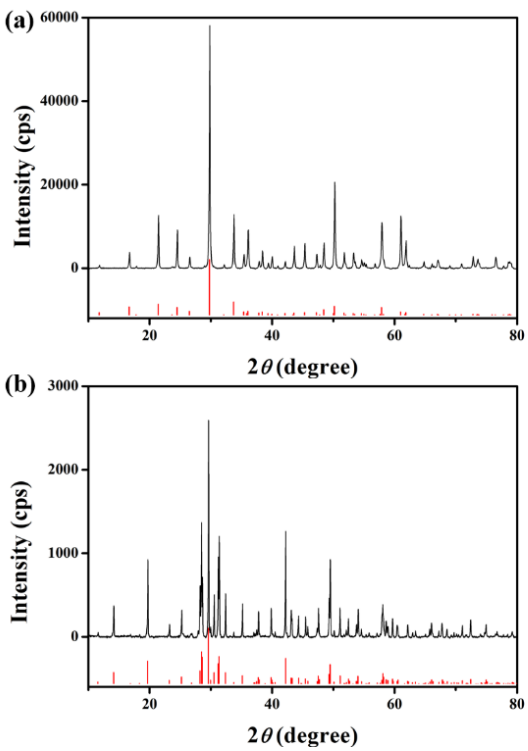

Figure 3. *p*-XRD patterns of the as-prepared (a) $Ag_2Sr(VO_3)_4$ and (b) $Sr(VO_3)_2$ compared with the standard patterns.

Figure 3a and 3b present the powder X-ray diffraction (*p*-XRD) patterns of the as-prepared $Ag_2Sr(VO_3)_4$ and $Sr(VO_3)_2$. All the observed diffraction peak positions of $Ag_2Sr(VO_3)_4$ and $Sr(VO_3)_2$ were respectively consistent with the standard *p*-XRD profiles in JCPDS database for $Ag_2Sr(VO_3)_4$ and $Sr(VO_3)_2$ (JCPDS-056-0127 for $Ag_2Sr(VO_3)_4$, *P4/nbm*, a = 10.6257 Å, b = 10.6257 Å, c = 4.9793 Å;

JCPDS-085-2440 for $Sr(VO_3)_2$, *Pnma*, a = 9.6660 Å, b = 3.6808 Å, c = 12.5290 Å), showing that the as-prepared samples were crystalized in single phases. Detailed rietveld refinements were also carried out to analyse the crystal structures of the as-prepared samples. The calculated patterns match our experimental data well, giving more evidence that the samples were well crystalized in single phase (as shown in Table 1, Fig S1 and S2).

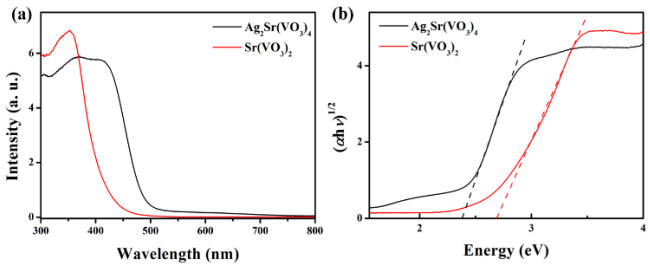

Figure 4. (a) UV-Vis absorption spectra of the as-prepared $Ag_2Sr(VO_3)_4$ and $Sr(VO_3)_2$ samples. (b) Tauc plot of $Ag_2Sr(VO_3)_4$ and $Sr(VO_3)_2$.

The ultraviolet-visible (UV-Vis) absorption spectra of as-prepared $Ag_2Sr(VO_3)_4$ and $Sr(VO_3)_2$ are shown in Figure 4a. Both of $Ag_2Sr(VO_3)_4$ and $Sr(VO_3)_2$ samples exhibit steep absorption edges with the wavelengths longer than 400 nm, suggesting that the materials can absorb visible light. The detailed the Tauc plots are presented in Figure 4b.[23] The band gaps of $Ag_2Sr(VO_3)_4$ and $Sr(VO_3)_2$ are determined as 2.4 and 2.7 eV, respectively. It was noticed that a absorption tail was observed from $Ag_2Sr(VO_3)_4$. This absorption is possibly caused by a small amount of metallic Ag, which is a normally detected by-product in the solid state synthesis of Ag based materials. In the X-ray photoelectron spectrum (XPS) of fresh $Ag_2Sr(VO_3)_4$ (as shown in Fig S6), both of Ag 3d5/2 and 3d3/2 peaks have small shoulder peaks with higher binding energy, which means metallic Ag exists on the $Ag_2Sr(VO_3)_4$ surface.[24]

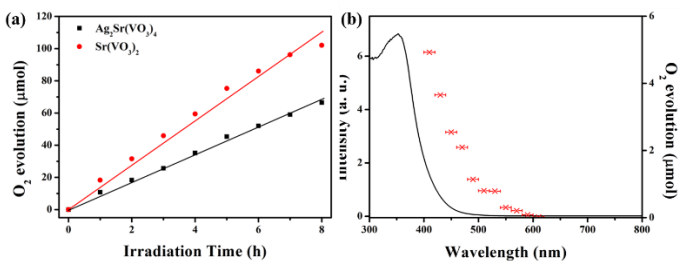

Figure 5. (a) Photocatalytic O_2 evolution from aqueous $Ce(SO_4)_2$ solution (270 mL of distilled water + 3 mmol of $Ce(SO_4)_2$) over the as-prepared $Ag_2Sr(VO_3)_4$ or $Sr(VO_3)_2$ samples (0.3 g) under the irradiation of visible light (λ > 400 nm, 300 W Xe arc lamp with L42 cut-off filter). (b) Wavelength dependence of O_2 evolution from aqueous $Ce(SO_4)_2$ solution containing the $Sr(VO_3)_2$ catalyst, showing good consistency with the absorption spectrum (reaction time: 3 h).

The photocatalytic O_2 evolution experiments over $Ag_2Sr(VO_3)_4$ or $Sr(VO_3)_2$ were firstly carried out by using $AgNO_3$ as sacrificial reagent, in which almost no O2 was detected. The samples changed color into brown-red after the experiments, and the p-XRD showed $AgVO_3$ was formed (as shown in Fig S4). In previous reports, $AgVO_3$ showed almost no water oxidation activity when $AgNO_3$ was used as a sacrificial agent.25 To avoid the formation of $AgVO_3$, other sacrificial agents, such as $Ce(SO_4)_2$ and $NaIO_3$ were employed as substitutes. The O_2 evolution from aqueous $Ce(SO_4)_2$ solution (3 mmol $Ce(SO_4)_2$ + 270 mL H_2O) containing 0.3 g of powder catalysts under the irradiation of visible light (λ > 400 nm, Xe arc lamp with L42 cut-off filter) is presented in Figure 5(a). O_2 gas continuously evolved over $Ag_2Sr(VO_3)_4$ or $Sr(VO_3)2$ for 8 hours. The O_2-evolution rates were 8.1 $\mu mol \cdot h^{-1}$ and 12 $\mu mol \cdot h^{-1}$ over $Ag_2Sr(VO_3)_4$ and $Sr(VO_3)_2$, respectively. It should be pointed out that the gradual decrease in O_2-evolution rate with increase in irradiation time was probably due to the surface reformation because the vanadate catalysts are slightly dissolvable in water. The XPS of $Ag_2Sr(VO_3)_4$ sample shows the Ag $3d_{5/2}$ and $3d_{3/2}$ peaks become broader and shift to higher binding energy after O2 evolution experiment, showing the formation of metallic Ag in the surface region (as shown in Fig. S6). However, after O_2 evolution, the samples exhibited no obvious changes in crystal structure (XRD patterns shown in Fig. S4 and Raman spectra shown in Fig. S8). Thus, the reformation should take place only in the surface region and the photocatalyst exhibits stable water oxidation activity in the long-term experiment (as shown in fig S7).

To confirm whether O_2 was generated by photocatalysis, reference experiments were carried out over the as-prepared vanadate catalysts. Dark experiments on $Ag_2Sr(VO_3)_4$ or $Sr(VO_3)_2$ showed no O_2 evolution when the irradiation light was off. Moreover, no O_2 gas was detected in the case that the aqueous $Ce(SO_4)_2$ solution was irradiated by visible light. The wavelength dependence of O_2 evolution performed with $Sr(VO_3)_2$ using a series of filters was measured and is shown in Figure 5b. The O_2-evolution rates under the irradiation of different wavelength light are consistent with the absorption spectrum. All these results support that the O_2 evolution was attributed to photocatalytic water oxidation.

The photocatalytic water oxidation experiments over $Ag_2Sr(VO_3)_4$ and $Sr(VO_3)_2$ presented good consistency with the result from theoretical calculation. Both of them can successfully oxidize water into O_2 in the present of sacrificial reagent. The difference in the photocatalytic activity between $Ag_2Sr(VO_3)_4$ and $Sr(VO_3)_2$ is probably attributed to their different electronic structures which is discussed in the previous section.

Table 2. The band gaps, surface areas, and photocatalytic O_2 evolution rates over $Ag_2Sr(VO_3)_4$ and $Sr(VO_3)_2$.

	Band gap (eV)	Surface area ($m^2 \cdot g^{-1}$)	O_2 evolution rate ($\mu mol \cdot h^{-1}$)
$Ag_2Sr(VO_3)_4$	2.4	1.2	8.1
$Sr(VO_3)_2$	2.7	1.6	12

In conclusion, to find new visible-light-sensitive photocatalysts, we theoretically studied the electronic structures of $Ag_2Sr(VO_3)_4$ and $Sr(VO_3)_2$. The CBM and VBM of $Ag_2Sr(VO_3)_4$ and $Sr(VO_3)_2$ provide favorable electronic structures for efficient migration of photo-generated charge carriers. Experimental results showed that $Ag_2Sr(VO_3)_4$ and $Sr(VO_3)_2$ can oxidize water into O_2 in the presence of sacrificial reagent at the O_2-evolution rates of 8.1 and 12 $\mu mol \cdot h^{-1}$, respectively. The improved photocatalytic O_2-evolution over $Ag_2Sr(VO_3)_4$ and $Sr(VO_3)_2$ is consistent with the theoretical implication.

Notes and references

[a] Catalytic Materials Group, Environmental Remediation Materials Unit, National Institute for Materials Science (NIMS), 1-1 Namiki, Tsukuba, Ibaraki 305-0044, Japan.
*E-mail: UMEZAWA.Naoto@nims.go.jp, ABE.Hideki@nims.go.jp
[b] PRESTO, Japan Science and Technology Agency (JST), 4-1-8 Honcho Kawaguchi, Saitama 332-0012, Japan.
[c] TU-NIMS Joint Research Center, School of Materials Science and Engineering, Tianjin University, 92 Weijin Road, Nankai District, Tianjin, P. R. China.
[d] International Center for Materials Nanoarchitectonics (WPI-MANA), National Institute for Materials Science (NIMS), 1-1 Namiki, Tsukuba, Ibaraki 305-0044, Japan.

Acknowledgement: This work was supported by Japan Science and Technology Agency (JST) and Precursory Research for Embryonic Science and Technology (PRESTO) program.

Electronic Supplementary Information (ESI) available: [details of any supplementary information available should be included here]. See DOI: 10.1039/c000000x/

1. M. R. Hoffmann, S. T. Martin, W. Y. Choi and D. W. Bahnemann, *Chem. Rev.*, 1995, 95, 69-96.
2. A. Kubacka, M. Fernandez-Garcia and G. Colon, *Chem. Rev.*, 2012, 112, 1555-1614.
3. H. Tong, S. Ouyang, Y. Bi, N. Umezawa, M. Oshikiri and J. Ye, *Adv. Mater.*, 2012, 24, 229-251.
4. Z. G. Zou, J. H. Ye, K. Sayama and H. Arakawa, *Nature*, 2001, 414, 625-627.
5. A. Kudo, *Int. J. Hydrogen Energy*, 2006, 31, 197-202.
6. F. E. Osterloh, *Chem. Mater.*, 2008, 20, 35-54.
7. A. Kudo and Y. Miseki, *Chem. Soc. Rev.*, 2009, 38, 253-278.
8. K. Maeda, *J. Photochem. Photobiol., C*, 2011, 12, 237-268.
9. A. Fujishima, X. Zhang and D. A. Tryk, *Surf. Sci. Rep.*, 2008, 63, 515-582.
10. X. Chen, S. Shen, L. Guo and S. S. Mao, *Chem. Rev.*, 2010, 110, 6503-6570.
11. A. Kudo, K. Omori and H. Kato, *J. Am. Chem. Soc.*, 1999, 121, 11459-11467.
12. G. Xi and J. Ye, *Chem. Commun.*, 2010, 46, 1893-1895.
13. Z. Yi, J. Ye, N. Kikugawa, T. Kako, S. Ouyang, H. Stuart-Williams, H. Yang, J. Cao, W. Luo, Z. Li, Y. Liu and R. L. Withers, *Nat. Mater.*, 2010, 9, 559-564.
14. Y. Bi, S. Ouyang, N. Umezawa, J. Cao and J. Ye, *J. Am. Chem. Soc.*, 2011, 133, 6490-6492.
15. D. J. Martin, N. Umezawa, X. Chen, J. Ye and J. Tang, *Energy Environ. Sci.*, 2013, 6, 3380-3386.
16. A. Walsh, Y. Yan, M. N. Huda, M. M. Al-Jassim and S.-H. Wei, *Chem. Mater.*, 2009, 21, 547-551.
17. N. Umezawa, O. Shuxin and J. Ye, *Phys. Rev. B*, 2011, 83.
18. J. M. Kahk, D. L. Sheridan, A. B. Kehoe, D. O. Scanlon, B. J. Morgan, G. W. Watson and D. J. Payne, *J. Mater. Chem. A*, 2014, 2, 6092-6099.
19. H. Kawazoe, H. Yanagi, K. Ueda and H. Hosono, *MRS Bulletin*, 2000, 25, 28-36.
20. P. Reunchan and N. Umezawa, *Phys. Rev. B*, 2013, 87, 245205.
21. D. F. Wang, J. W. Tang, Z. G. Zou and J. H. Ye, *Chem. Mater.*, 2005, 17, 5177-5182.
22. R. W. G. Wyckoff, *Am. J. Sci.*, 1925, 10, 107-118.
23. M. A. Butler, *J. Appl. Phys.*, 1977, 48, 1914-1920.
24. H. Cheng, B. Huang, P. Wang, Z. Wang, Z. Lou, J. Wang, X. Qin, X. Zhang and Y. Dai, *Chem. Commun.*, 2011, 47, 7054-7056.
25. R. Konta, H. Kato, H. Kobayashi and A. Kudo, *Phys. Chem. Chem. Phys.*, 2003, 5, 3061-3065.